

## GRAIN BOUNDARY DEPENDENT CREEP BEHAVIOUR OF INCONEL 718

W. CHEN and M. C. CHATURVEDI

Department of Mechanical Engineering, University of Manitoba, Winnipeg, Manitoba R3T 2N2, Canada

(Received 14 August 1992; accepted in revised form 5 January 1993)

**Abstract**—Inconel 718 specimens with similar grain boundary precipitates but with different sizes of  $\gamma''$  strengthening precipitates have been creep deformed at 770 MPa and 625°C. It has been observed that the steady state creep rate of the materials is independent of the size of the  $\gamma''$  precipitates present in the grain for precipitate dimensions from 17.3 to 26.2 nm. This is contrary to results for material with clean grain boundaries which show a distinct minimum creep rate for 22 nm  $\gamma''$  precipitates. This unusual behaviour contradicts the generally held belief that creep deformation in the power-law region is controlled by deformation in the bulk grain material with grain boundaries making only a minor contribution through sliding. It is suggested that for Inconel 718 specimens containing  $\delta$  phase grain boundary precipitates the creep rate is determined by deformation in the grain boundaries.

**Résumé**—Différents échantillons d'Inconel 718 contenant les mêmes précipités aux joints de grains mais différentes tailles de précipités durcissants  $\gamma''$ , ont été déformés par fluage à 625°C sous 770 MPa. Les observations montrent que le taux de fluage en régime permanent des matériaux est indépendant de la taille des précipités  $\gamma''$  présents dans le grain lorsque leur dimension varie de 17.3 à 26.2 nm. Ces résultats sont contraires aux observations sur des matériaux possédant des joints de grains propres qui montrent un taux minimum pour des précipités  $\gamma''$  de 22 nm. Ce comportement inhabituel contredit la croyance générale, à savoir que le fluage associé à une loi de puissance est contrôlé par une déformation intra-granulaire avec seulement une contribution mineure du glissement des joints de grains. Il est suggéré que pour des échantillons d'Inconel 718 contenant des précipités intergranulaires de phase  $\delta$ , le taux de déformation en fluage soit régi par la déformation des joints de grains.

### INTRODUCTION

The effect of grain boundary strengthening through precipitation on the creep resistance of a material in the power-law dislocation creep region has not received much attention in past years [1] although its effect on the mechanism of creep fracture has been extensively studied [1–4]. This may be because of the generally held belief that creep behaviour in the power-law dislocation region is rate-controlled by the grain material and that grain boundary sliding makes only a minor contribution to the overall creep rate [1]. However, a few recent results have indicated that the presence of precipitates at grain boundaries not only influences the creep fracture of the material, but also significantly influences the creep deformation mechanism [5–8]. Since only a few studies have been carried out and are in some aspects contradictory, especially in the precipitation strengthened alloys, studies were initiated to determine the effect of grain boundary precipitates on the creep deformation of Inconel 718. This communication presents preliminary results of the investigation carried out so far.

### EXPERIMENTAL METHODS

The chemical composition of Inconel 718, as determined by mass spectroscopy by Arrow Laboratory, Wichita, Kansas (U.S.A.), is given in Table 1. A 2.54 mm thick sheet of the alloy was cold-rolled to a thickness of 1.4 mm and was then machined into flat samples with a gauge dimension of 1.3 mm  $\times$  5.3 mm  $\times$  25.4 mm. The samples were then variously heat treated

to produce different states of dispersion of the disc-shaped strengthening precipitates of tetragonal  $\text{Ni}_3\text{Nb}$  phase  $\gamma''$  and spherical precipitates of  $\text{L1}_2$  phase  $\gamma'$ , as well as a constant size grain boundary precipitate of the  $\delta$ - $\text{Ni}_3\text{Nb}$  phase which has an orthorhombic structure. The microstructures of heat treated samples were examined by a JEOL 840 Analytical Scanning Electron Microscope and a JEOL 2000FX Analytical TEM/STEM. The precipitate particle size was measured using enlarged micrographs on a Leitz Image Analyzer. The creep tests were carried out at 625°C and at a constant stress of 770 MPa on a Denison constant stress creep machine. During the creep tests the temperature was controlled within  $\pm 3^\circ\text{C}$  and a flow of argon through the test chamber was maintained. Creep strain was recorded on a strip chart recorder.

### RESULTS AND DISCUSSION

The creep samples were heat treated in accordance with the following scheme which is based on the work of other inves-

Table 1. Chemical compositions of Inconel 718 (wt %)

Element	%	Element	%
C	0.03	Mo	3.07
Fe	19.24	Nb + Ta	4.94
Ni	52.37	Mn	0.007
Cr	18.24	S	0.007
Al	0.25	Si	0.30
Ti	0.97	Cu	0.04

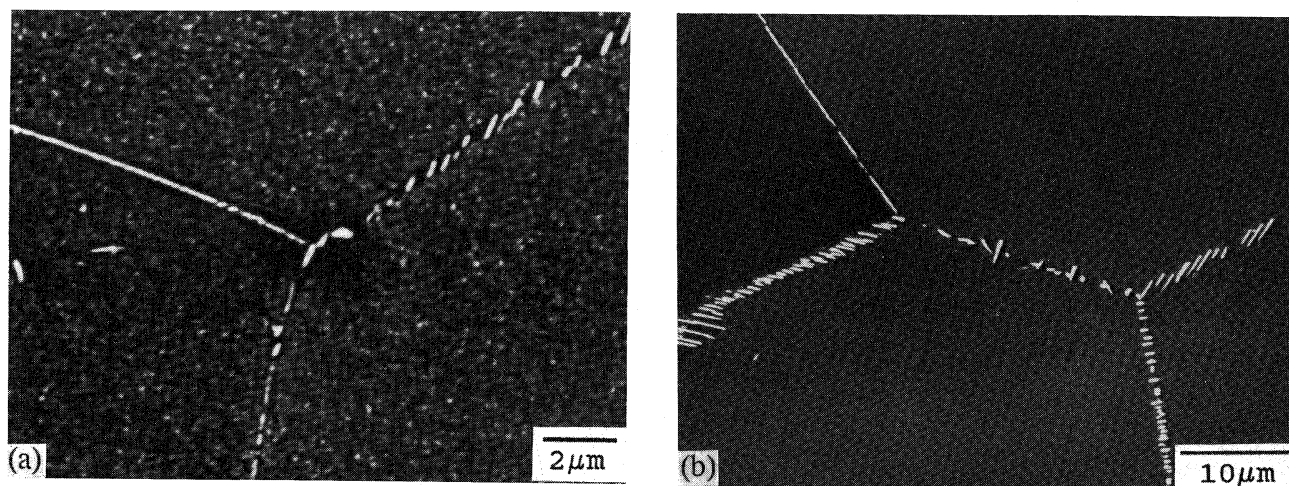


Fig. 1. SEM images showing the microstructures (a) after furnace cooling to 725°C after solid solution treatment at 1020°C for 4 h; (b) after partial solid solution at 925°C for 1 h.

tigators [9–11]: solution heat treatment at 1020°C for 4 h, furnace cooling down to 725°C at 50°C h<sup>-1</sup>, partial solution treatment at 925°C for 1 h, air cooling to room temperature, followed by aging at 725°C for different times. The solution treatment at 1020°C for 4 h caused the dissolution of all the precipitates, with the exception of a small amount of MC carbide, without inducing excessive grain growth. The subsequent furnace cooling produced precipitates of  $\delta$ -Ni<sub>3</sub>Nb phase at grain boundaries, as shown in Fig. 1(a) which is the SEM micrograph of an etched specimen. This micrograph also shows that furnace cooling introduces relatively large precipitates of  $\gamma''$  and  $\gamma'$  phases in the grain interiors. The second solution heat treatment at 925°C for 1 h caused a dissolution of ( $\gamma' + \gamma''$ ) precipitates in the grain interiors and a growth of the  $\delta$  precipitates at the grain boundaries as shown in the SEM micrograph in Fig. 1(b). Since the precipitation of  $\delta$  phase in Inconel 718 occurs in the temperature range 820–1010°C [12], the subsequent aging at 725°C did not cause any change in the size of precipitates at grain boundaries. This is shown in Figs 2(a) and (b) which are the SEM micrographs of a specimen aged for 25 and 50 h at

725°C after the second solution treatment at 925°C. The dark field TEM micrographs of these two specimens are shown in Figs 3(a) and (b) where the average diameter of  $\gamma''$  discs was measured to be 17.3 and 21.2 nm, respectively. Therefore, it is concluded that the heat treatment described above produces material that has the same size of  $\delta$  phase precipitates at grain boundaries and different sizes of  $\gamma''$  phase precipitates depending upon the length of aging at 725°C. The average grain size of the material remained constant at 60  $\mu$ m.

The variation in creep rate with creep strain for various specimens with  $\gamma''$  precipitate discs of different diameter is shown in Fig. 4. For a clearer presentation of results without undue overlapping of curves, this figure is divided into two halves. All seven curves show a steady state creep rate with increasing creep strain. The value of steady state creep rate,  $\dot{\epsilon}_s$ , for the specimen with the smallest and the largest precipitate particles is greater than that observed in other specimens. The steady state creep rate,  $\dot{\epsilon}_s$ , is also observed to be the same as the minimum creep rate,  $\dot{\epsilon}_m$ , with the exception of specimen 4, where the average diameter of the  $\gamma''$  discs is 21.4 nm, the value

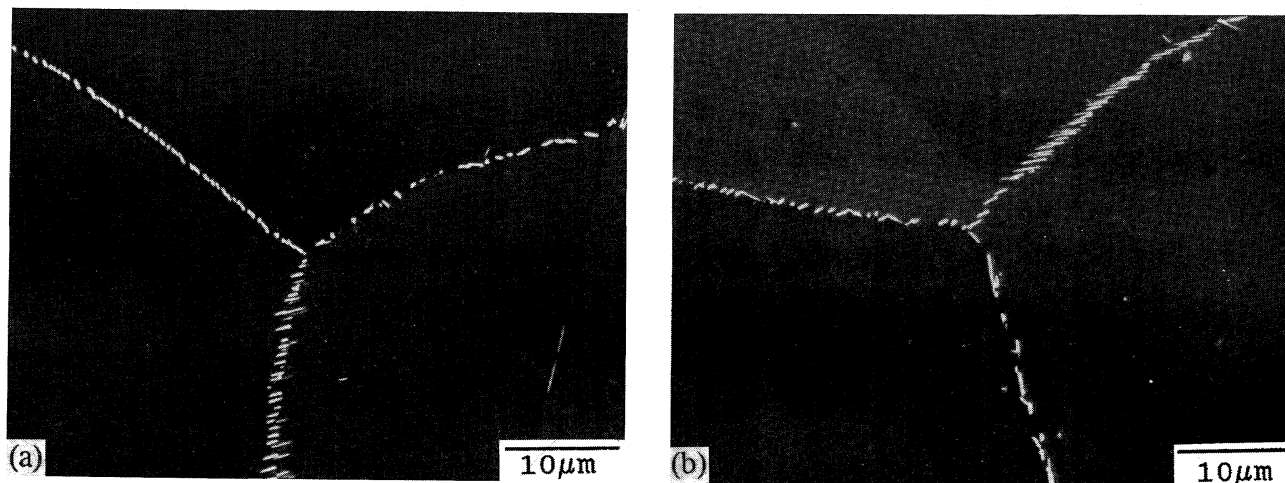


Fig. 2. SEM images of precipitates of the  $\delta$  phase at grain boundaries. The materials have been aged at 725°C for 25 h (a) and 50 h (b).

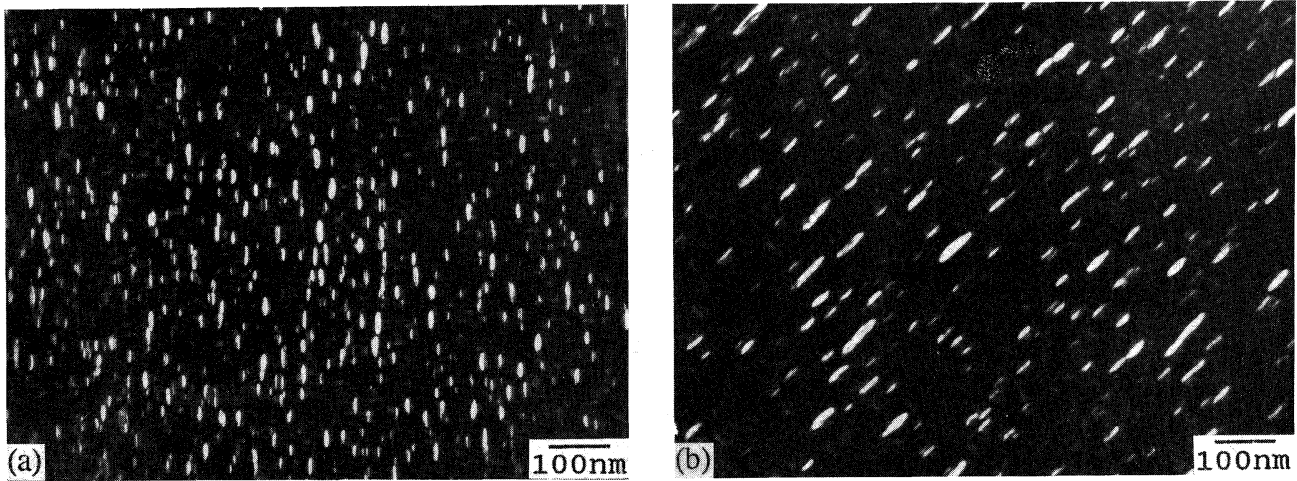


Fig. 3. Dark field TEM images of  $\gamma''$  of grain interiors. The materials have been aged at 725°C for 25 h (a) and 50 h (b). In (a)  $d_{\gamma''} = 17.3$  nm, in (b)  $d_{\gamma''} = 21.2$  nm.

of the minimum creep rate is significantly smaller than the steady state creep rate. The validity of the existence of this sharp minimum was established by duplicate tests. It should be noted that specimens with 17.3 and 21.2 nm  $\gamma''$  precipitates exhibit a significant steady state creep region and in the specimen with 21.2 nm  $\gamma''$  the sharp minimum in creep rate occurred before the steady state stage was reached. The values of steady state creep rate observed in various specimens are plotted against average diameter of  $\gamma''$  discs in them in Fig. 5. It is seen that the value of steady state creep rate acquires a constant value when the average diameter of the  $\gamma''$  discs reaches 17.3 nm and increases again when it is 26.2 nm.

The creep behaviour of specimens with clean grain bound-

aries under the test conditions similar to those used in this study has been characterized by Han and Chaturvedi as power-law dislocation creep with a true stress exponent of about 5 [13, 14]. The dependence of steady state creep rate on the size of  $\gamma''$  in specimens tested at 625°C and 765 MPa, as reported by Chaturvedi and Han [14], is included in Fig. 5. It can be seen that the creep rate of the material with clean grain boundaries is strongly dependent upon the size of  $\gamma''$  precipitates. Such a dependence of steady state creep rate on the precipitate particle size has been observed in the applied stress range 620–815 MPa and also reported in Cu–Co alloys by Threadgill and Wilshire [15]. However, the results of this study show that the presence of about 5  $\mu\text{m}$  size  $\delta$  precipitates at the grain boundaries makes

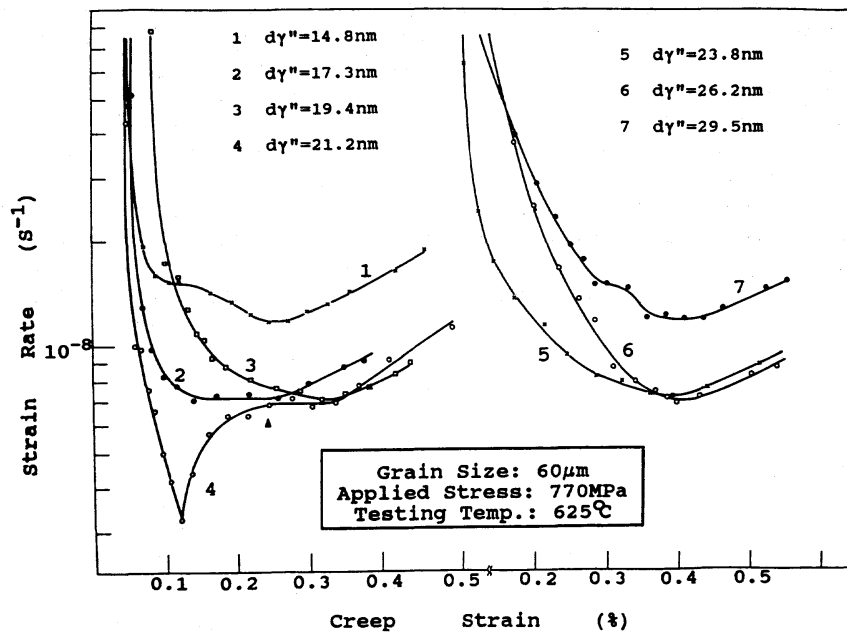


Fig. 4. Change of creep rate with creep strain for the materials with various sizes of  $\gamma''$ . The creep test was conducted at 770 MPa and 625°C.

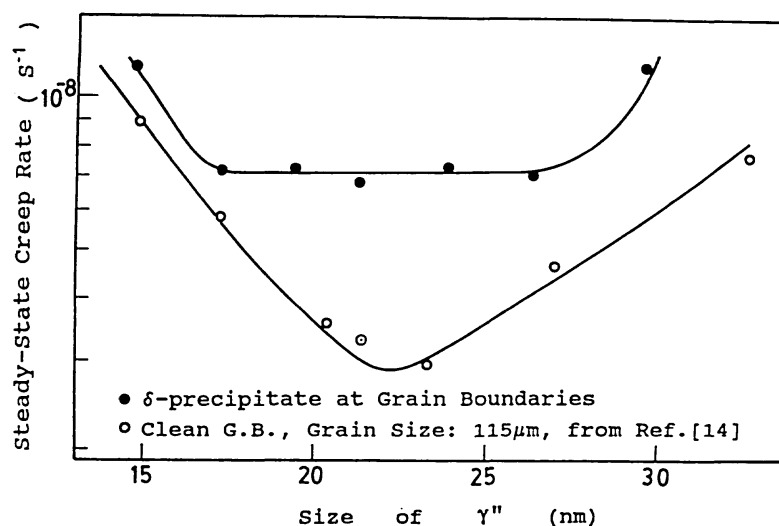


Fig. 5. Dependence of steady state creep rate on the size of  $\gamma''$ .

the minimum creep rate,  $\dot{\epsilon}_m$ , independent of the  $\gamma''$  precipitate size over a certain size range. That is, the values of the steady state creep rate are independent of the strength of the grain material unlike that generally believed for creep in the power-law dislocation creep region. It should also be noted that the values of steady state creep rate in material with  $\delta$  precipitates at the grain boundary are significantly higher than those observed in the material with clean grain boundaries. It has been reported that in order to provide creep resistance the precipitates must be smaller than 10 nm or larger than 100  $\mu m$  [4, 16]. The present results are not only consistent with this but also suggest that the presence of 5 nm  $\delta$  particles at the grain boundaries weaken them. Therefore, for this material, creep seems to be controlled by the grain boundary deformation, with the exception of material where 21.2 nm diameter discs of the  $\gamma''$  phase are present in the grain.

The unusual creep rate curve for the material with an average of 21.2 nm diameter discs of  $\gamma''$  particles in it is somewhat similar to that observed by Matsuo *et al.* [8] and Terada *et al.* [17] in a single phase Ni-20Cr-B alloy. They found that the creep curves consisted of two stages: primary and tertiary. In the tertiary stage, the creep rate increased rapidly both in the beginning and towards the fracture stage but increased relatively slowly in the middle. They suggested that the onset of the tertiary creep and the acceleration of the creep rate are due to dynamic recrystallization and to the sub-grain evolution accompanied by the increase in misorientation across sub-boundaries. They also concluded that the increase in misorientation would cause the decrease in creep resistance. In the present two phase alloy, recrystallization and sub-grain evolution did not occur and this hypothesis may, therefore, not be applicable. Other explanations for the shape of plot 4 in Fig. 4 could be void formation around grain boundary precipitates or a degradation of microstructure during creep tests. However, neither degradation of microstructure nor voids on grain boundaries are observed neither in specimen creep deformed to the minimum creep rate stage nor in the one deformed to the steady state stage. An

example of this is shown in Fig. 6(a) which is the TEM microstructure of a specimen deformed to the stage marked by "▲" in plot 4 in Fig. 4. The SEM micrograph of the same specimen is shown in Fig. 6(b) which shows that voids are not present at the grain boundaries. However, in the specimen deformed to the tertiary stage, voids were observed around  $\delta$  precipitates at the grain boundaries, as shown in Fig. 7. Therefore, it is probable that the creep deformation of material with 5  $\mu m$  size  $\delta$  precipitates at the grain boundaries does involve grain boundary sliding and void formation, except that the voids are too small to be observed in a specimen deformed to the stage where a minimum in creep rate-creep strain curve is observed. However, it is also probable that creep deformation in this material, where the  $\gamma''$  particle size is such that it produces maximum strengthening [14], is controlled by some unexplained precipitate-particle interaction which causes a significant reduction in the minimum creep rate from the steady state creep rate.

The high creep rate beyond the region over which the creep rate is independent of the size of  $\gamma''$  discs is due to the level of applied stress. It was found that the applied stress of 770 MPa is somewhat greater than the flow stress of the material with  $\gamma''$  discs of 14.8 and 29.5 nm diameter in them, which was observed to be 740 and 750 MPa, respectively. Under these circumstances creep deformation will be determined by the strength of the grain material.

## SUMMARY AND CONCLUSION

Inconel 718 specimens with similar size of grain boundary precipitates (5  $\mu m$ ) but with different sizes of  $\gamma''$  strengthening precipitates have been creep deformed. It has been observed from creep tests at 770 MPa and 625°C that the steady state creep rate of the materials is independent of the size of the  $\gamma''$  precipitates present in the grain for precipitate dimensions from 17.3 to 26.2 nm. This is contrary to the results for material with

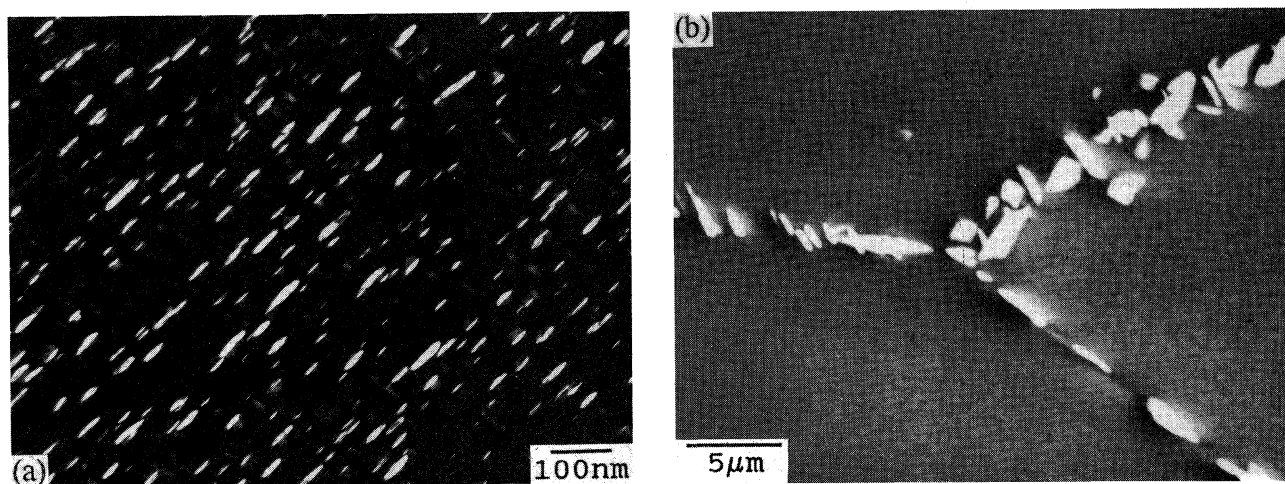


Fig. 6. Microstructures of the sample with  $d_{\gamma''} = 21.2$  nm interrupted from the creep test at the position marked "▲" in Fig. 4. (a) Dark field TEM image of  $\gamma''$ . The size of  $\gamma''$  is maintained during the test; (b) SEM image of the grain boundary microstructure. No creep voids have been observed.

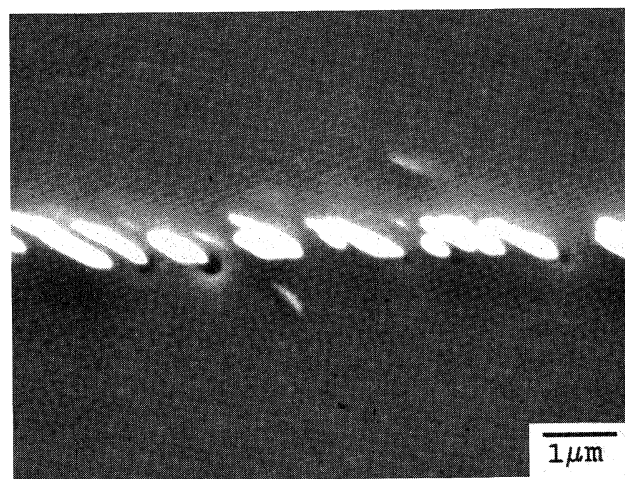


Fig. 7. Isolated creep voids observed around  $\delta$  phase precipitates at grain boundaries in specimen 4 deformed to the end of steady state creep stage.

clean grain boundaries which show a distinct minimum steady state creep rate for a specimen with 22 nm size  $\gamma''$  precipitates in it. In addition, the value of the  $\gamma''$  precipitate size independent steady state creep rate is significantly larger than those observed in material with clean grain boundaries. Therefore, it is concluded that the presence of 5  $\mu\text{m}$  size  $\delta$  phase precipitates at grain boundaries weakens them and the creep deformation is controlled by the creep deformation of grain boundaries and not grain material.

## REFERENCES

1. J. Cadek, *Creep in Metallic Materials*, pp. 246–270. Elsevier Science, New York (1988).
2. M. Ashby, C. Gandhi and D. M. R. Taplin, *Acta Metall.* **27**, 699 (1979).
3. C. Gandhi and M. F. Ashby, *Acta Metall.* **27**, 1565 (1979).
4. A. S. Argon, *Recent Advances in Creep and Fracture of Engineering Materials and Structures* (edited by B. Wilshire and D. R. J. Owen), pp. 1–52. Pineridge Press, Swansea (1982).
5. F. T. Furillo, J. M. Davidson, J. K. Tien and L. A. Jackman, *Mater. Sci. Engng* **39**, 267 (1979).
6. J. Zhang, P. Li, W. Chen and J. Jin, *Scr. Metall.* **23**, 547 (1989).
7. J. Zhang, W. Chen, Z. Cao and R. Tanaka, *Tetsu To Hagane* **75**, 545 (1989).
8. T. Matsuo, K. Nakajima, Y. Terada and M. Kikuchi, *Mater. Sci. Engng A146*, 261 (1991).
9. E. Campo, C. Turco and V. Catena, *Metall. Sci. Tech. J. TEKSID (Italy)* **3**, 16 (1985).
10. A. K. Koul, P. Au, N. Bellinger, R. Thamburaj, W. Wallace and J.-P. Immarrigeon, *Superalloys 1988* (edited by S. Reichman *et al.*), p. 3. The Metallurgical Society (1988).
11. J. W. Brooks and P. J. Bridges, *Superalloys 1988* (edited by S. Reichman *et al.*), p. 33. The Metallurgical Society (1988).
12. A. Oradei-Basile and J. F. Radavich, *Proceedings of the International Symposium on the Metallurgy and Applications of Superalloys 718, 625 and Various Derivatives*, 23–26 June 1991, Pittsburgh, Pennsylvania, p. 325 (1991).
13. Y. Han and M. C. Chaturvedi, *Mater. Sci. Engng* **89**, 25 (1987).
14. M. C. Chaturvedi and Y. Han, *Mater. Sci. Engng* **89**, L7 (1989).
15. P. L. Threadgill and B. Wilshire, *Metal Sci.* **8**, 117 (1974).
16. J. Rosler and A. G. Evans, *Mater. Sci. Engng A153*, 438 (1992).
17. Y. Terada, T. Matsuo and M. Kikuchi, 123rd Committee on Heat Resisting Metals and Alloys Report 31, p. 93 (1990).